



Effect of freeze-thaw cycles on soil engineering properties of reservoir bank slopes at the northern foot of Tianshan Mountain

Zi-peng QIN, Yuan-ming LAI, Yan TIAN, Ming-yi ZHANG

View online: <https://doi.org/10.1007/s11629-020-6215-z>

Articles you may be interested in

[Mechanical and acoustic emission characteristics of anhydrite rock under freeze-thaw cycles](#)

Journal of Mountain Science. 2023, 20(1): 227 <https://doi.org/10.1007/s11629-022-7661-6>

[Water migration in subgrade soil under seasonal freeze-thaw cycles in an alpine meadow on the Qinghai-Tibet Plateau](#)

Journal of Mountain Science. 2022, 19(6): 1767 <https://doi.org/10.1007/s11629-021-7270-9>

[Effect of freeze-thaw cycles on mechanical behavior of clay-gravel mixtures](#)

Journal of Mountain Science. 2022, 19(12): 3615 <https://doi.org/10.1007/s11629-022-7317-6>

[Seasonal freezing-thawing process and hydrothermal characteristics of soil on the Loess Plateau, China](#)


Journal of Mountain Science. 2021, 18(11): 3082 <https://doi.org/10.1007/s11629-020-6599-9>



[Effects of freezing-thawing on the engineering performance of core wall soil materials of a dam in the process of construction](#)


Journal of Mountain Science. 2020, 17(11): 2840 <https://doi.org/10.1007/s11629-020-6264-3>


Original Article

Effect of freeze-thaw cycles on soil engineering properties of reservoir bank slopes at the northern foot of Tianshan Mountain

QIN Zi-peng^{1,2}  <https://orcid.org/0000-0002-9561-8772>; e-mail: qinzipeng@lzb.ac.cn

LAI Yuan-ming^{1,2*}  <https://orcid.org/0000-0003-0535-1355>;  e-mail: ymlai@lzb.ac.cn

TIAN Yan³  <https://orcid.org/0000-0001-6350-3041>; e-mail: tianyan19@lzu.edu.cn

ZHANG Ming-yi^{1,2}  <https://orcid.org/0000-0001-5501-8767>; e-mail: myzhang@lzb.ac.cn

*Corresponding author

¹ State Key Laboratory of Frozen Soil Engineering, Northwest Institute of Eco-Environment and Resources, Chinese Academy of Sciences, Lanzhou 730000, China

² University of Chinese Academy of Sciences, Beijing 100049, China

³ College of Civil Engineering and Mechanics, Lanzhou University, Lanzhou 730000, China

Citation: Qin ZP, Lai YM, Tian Y, et al. (2021) Effect of freeze-thaw cycles on soil engineering properties of reservoir bank slopes at the northern foot of Tianshan Mountain. *Journal of Mountain Science* 18(2). <https://doi.org/10.1007/s11629-020-6215-z>

© Science Press, Institute of Mountain Hazards and Environment, CAS and Springer-Verlag GmbH Germany, part of Springer Nature 2021

Abstract: The instability of soil bank slopes induced by freeze-thaw cycles at the northern foot of Tianshan Mountain is very common. The failure not only caused a large amount of soil erosion, but also led to serious reservoir sedimentation and water quality degradation, which exerted a lot of adverse effects on agricultural production in the local irrigation areas. Based on field investigations on dozens of irrigation reservoirs there, laboratory tests were carried out to quantitatively analyze the freeze-thaw effect on the soil engineering characteristics to reveal the facilitation on the bank slope instability. The results show that the softening characteristics of the stress-strain curves gradually weaken, the effective cohesions decline exponentially, the seepage coefficients enlarge, and the thermal conductivities decrease after 7 freeze-thaw cycles. The freeze-thaw effect on the specimens with low confining pressures, low dry densities and high water contents is more significant. The water migration and the phase transition between water and ice result in the variations of the soil internal microstructures, which

is the main factor affecting the soil engineering characteristics. Sufficient water supply and the alternation of positive and negative temperatures at the reservoir bank slopes in cold regions make the water migration and phase transition in the soil very intensely. It is easy to form a large number of pores and micro cracks in the soil freezing and thawing areas. The volume changes of the soil and the water migration are difficult to reach a dynamic balance in the open system. Long-term freeze-thaw cycles will bring out the fragmentation of the soil particles, resulting in that the micro cracks on the soil surfaces are developing continuously. The soil of the bank slopes will fall or collapse when these cracks penetrate, which often happens in winter there.

Keywords: Mechanical properties; Seepage coefficient; Thermal conductivity; Micro structure; Freeze-thaw cycles; Reservoir bank slope

1 Introduction

Freeze-thaw cycles are caused by the periodic

Received: 19-May-2020

Revised: 03-Sep-2020

Accepted: 10-Oct-2020

positive and negative alternation of temperatures, and make the hydrous soil constantly change phase and displacement, which is one of the most common geological disasters in the active layer of the permafrost and seasonally frozen soil regions (Kraatz et al. 2020; Wu et al. 2020; Yang et al. 2020; Zhang et al. 2020). The pore structures of the soil are closely related to its engineering properties. It is generally believed that the freeze-thaw cycles can change the soil engineering properties by altering the pore structures (Wang, et al. 2020). In fact, they not only transform the micro structures, but also lead to changes in soil physical, mechanical, water physical, chemical and biological communities (Chen et al. 2020; Chen et al. 2020; Du et al. 2020; Hou et al. 2020; Liu et al. 2020; Sutton and Price 2020; Wang et al. 2020; Yuan et al. 2020; Zhang et al. 2020). These will affect the soil engineering characteristics. The freeze-thaw cycles can increase the number of macro pores and make the micro cracks gradually appear and expand in the soil, resulting in the degradation of the mechanical properties (Liu et al. 2020; Lu et al. 2020; Tian et al. 2020; Zhang et al. 2020; Zhou et al. 2020; Zhou et al. 2020). The phenomenon is more significant in the soil with high water contents (Wang et al. 2020). Simultaneously, the soil stress-strain behaviors will change (Lei et al. 2019; Liu et al. 2020; Qu et al. 2020). When the bank slope is damaged by freeze-thaw cycles, not only the mechanical and deformation properties of the soil are affected, but also the permeability and thermal conductivity will be changed. The freezing and thawing process can cause water migration in the soil (Chen et al. 2020; Wang et al. 2020), and change its hydraulic properties and infiltration characteristics (Ozgul et al. 2011; Roy et al. 2020; Yang et al. 2020), which will raise the soil permeability coefficients in the freeze-thaw zones significantly (Benson et al. 1995; Yang et al. 2020). It is easy to initiate seepage failure (Dalla Santa, et al. 2019). The thermal conductivity is one of the important parameters related to the soil heat exchange (Li et al. 2019) and the freezing depth and the freeze-thaw intensity are bound up with it (Wang et al. 2020). The change of the soil engineering characteristics directly affects the bank slope stability (Kawamura and Miura 2013; Qi et al. 2006; Qu et al. 2019), and the long-term freeze-thaw action can significantly promote its instability (Li et al. 2020; Xu et al. 2018).

The freeze-thaw failure is a result of the

moisture-heat-stress coupling effects and it needs to be understood from multiple perspectives. Most of the above-mentioned researches only focus on one kind of soil performance, which is not enough to understand the influence of freeze-thaw cycles on soil engineering performance. The above analyses indicate that the freeze-thaw cycles can obviously degrade soil engineering properties and can exacerbate the risk of the reservoir bank slope instability. Therefore, it is necessary to consider their effect in the soil parameter selection when carrying out engineering practices in cold regions. To quantitatively analyze and reveal the freeze-thaw effects on the soil engineering properties, indoor tests are carried out on the basis of a large number of field investigations. The evolution law of soil physical and mechanical properties of the reservoir bank slope under freeze-thaw cycles is studied. The research can provide basic data for further study on the instability mechanism of the soil bank slopes in cold regions and supply some references for explaining their failure under freeze-thaw cycles.

2 Study Area

The reservoir soil bank slopes at the northern foot of Tianshan Mountain suffer from serious freeze-thaw cycle damage, resulting in many collapses every year. The northern foot of Tianshan Mountain is the most developed area in the Xinjiang Uygur Autonomous Region of China with the most intensively industrial and agricultural production. It is not only convenient for transportation, but also rich in land resources and sufficient light and heat resources, which is suitable for large-scale industrial and agricultural production. However, the water resource shortage directly restricts the local economic development, owing to its location in the arid and semi-arid region. It is arid and rainless in summer, and the annual evaporation is much larger than the rainfall. Agricultural development highly depends on artificial irrigation. The agricultural irrigation water consumption is huge, and the irrigation water source is mostly from snow melts in the high mountains (Zhao et al. 2018). Damming and impoundment along the rivers at the upstream of the irrigation areas is an effective way to solve the problem of irrigation water (Qin et al. 2019). It is frigid in winter. The freeze-thaw disasters occur frequently at the beginning and end of

winter, which poses a great threat to the operation and management of water conservancy projects. The soil bank slopes of the irrigation reservoirs often collapse in winter and spring, which leads to a large amount of soil and water loss, serious reservoir siltation and degraded water quality (Zhang et al. 2020).

Field investigations of dozens of irrigation reservoirs there were carried out from 2018 to 2020, and it were found that the soil bank slopes collapsed severely in winter and spring, leaving many smooth fracture surfaces. Due to the abundant water sources and the rich groundwater contents, the water migrates violently from bottom to top under the external evaporation. The water contents of the fracture surfaces at the middle and lower parts of the bank slopes are still high although the temperature in summer is as high as about 40°C. It is difficult to find cracks in these places. However, after entering winter, a large number of cracks appear. The continuously increasing, widening and expanding of cracks in the freeze-thaw environment often lead to bank slope collapses. Fig. 1 shows a large number of cracks and collapses on the soil bank slope at the northern foot of Tianshan Mountain in winter.

In April 2019, a large-scale collapse was found, as shown in Fig.1a, and the bank slope retreated up to about 2.5m. Two new fracture surfaces at its lower part are selected for long-term observation as shown by the red rectangular frames in Fig.1a. The two fracture surfaces are flat and smooth, and the soil is dense, even and wet. The surface soil (10cm depth from the surface) was tested for several times from June to August in 2019, the water content remained about 15%, and no cracks were found there. By October, the agricultural irrigation water was basically stopped, the water level of the reservoir increased, the soil water content increased to about 17%, and there were no cracks found on the surfaces yet. In November, there were many times of violent alternation of positive and negative temperatures, and a large number of micro cracks appeared there. In January 2020, the micro cracks further increased, widened, and extended. The maximum crack width reached about 4mm, and the selected observation

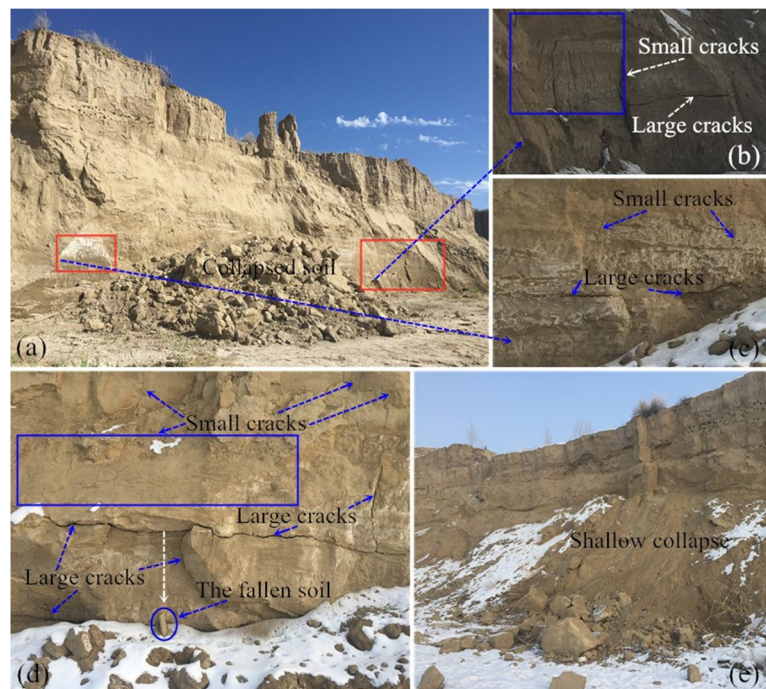


Fig. 1 The cracks and collapses on the soil bank slope of irrigation reservoirs at the northern foot of Tianshan Mountain in winter. (a) The smooth straight facade formed by the collapsed bank slope (photographed in June 2019). (b) and (c) A large number of cracks appear on the smooth vertical surfaces (in Fig. 1a) in winter (photographed in January 2020). (d) The cracks at the middle and lower part of another soil bank slope section (photographed in January 2020). (e) The collapse in winter without snow melting (photographed in January 2020).

surfaces became rough, showing an obvious freeze-thaw erosion phenomenon, as shown in Fig.1b and c. That is common at the middle and lower parts of the slope. The soil will fall or collapse due to continuous cracking in the process of external environment variations, as shown in Fig.1d and e. Similar phenomena have appeared in the laboratory freeze-thaw model test of the reservoir bank slope, as shown in Fig. 2a. The geometric dimension ratio of the prototype and model is 10:1, and the setting of temperature and soil parameters is basically consistent with the prototype. A large number of cracks appear at its middle and lower parts after 2 freeze-thaw cycles, which expand with the increasing cycles, as shown in Fig. 2b, c and d.

The study area is located at Liugou Reservoir area. The reservoir is in the upstream of Kuitun irrigation area of the seventh division of the Xinjiang Production and Construction Corps at the northern foot of Tianshan Mountain, as shown in Fig. 3a. It is a large-scale injected plain reservoir with a capacity of 102 million m³, which is mainly used for irrigation.

The water source is from Sikeshu River and Gultu River.

The formation lithology of the reservoir area (The altitude is 350-400m) is covered by Quaternary middle lower Pleistocene and Holocene horizontal fine soil desert stratum. The lithology is dominated by clay, loam, sandy loam and silty fine sand layer, with medium fine sand mixed with gravel layer locally, with a total thickness of over 100m.

The area is in the center of Eurasia and far away from the ocean, with a continental north temperate climate. The annual average temperature is 6.5°C. The coldest month is January (The average temperature is -18°C and the minimum temperature is -42.3°C), and the hottest month is July (The average temperature is 25.7°C and the maximum temperature is 42.1°C). The annual average precipitation and evaporation are 161.5mm and 1785mm, respectively. The maximum snow depth is 36 cm in the northern plain areas and 60 cm in mountain areas.

The soil bank slopes with a length of about 16.5 kilometers located in the east and southeast sides of the reservoir are unprotected. The landslides and collapses often occur there. The slope within 1km from the south of the east dam is taken as the main research object, as shown in Fig.3c and d. Its average height is about 10m, which is developed in coherent sandy silty sediment. Its upper part is almost vertical with a height of 4-5m, and the lower part is steep with an inclination in the range of 50°-80° mostly and close to 90° in some slope sections. The bank slope there has accumulated to retreat more than 100m in the past 40 years.

3 Materials and Methods

3.1 Materials

The soil specimens are taken from the selected research section of Liugou Reservoir, with the specific gravity of 2.69, liquid limit of 24.2%, plastic limit of 14.6% and plastic index of 9.6. Its particle grading is shown in Fig. 4. The clay content of the soil specimen with particle diameters less than 0.005mm is less than 10%, which belongs to sandy silt. The soil

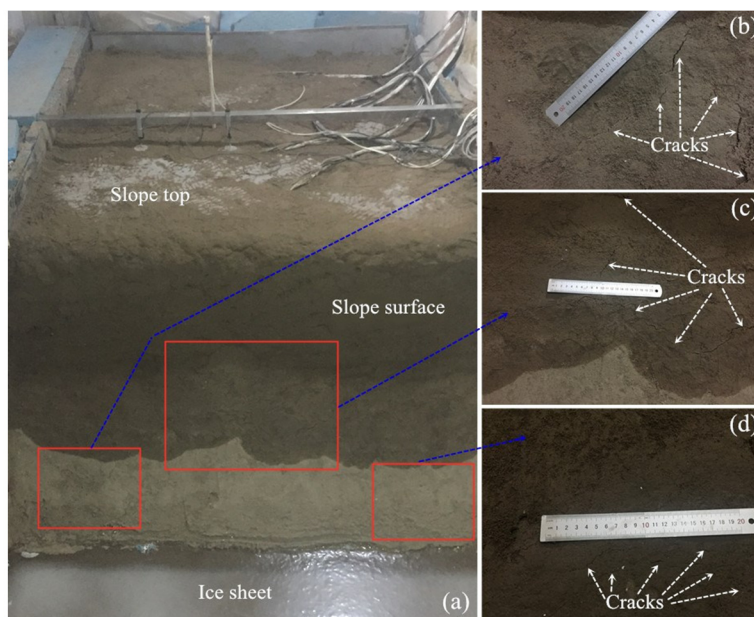


Fig. 2 The distribution of slope cracks of the reservoir bank in the indoor model during freezing and thawing processes. (a) The indoor bank slope model. (b), (c) and (d) A large number of cracks appeared on the model slope after freeze-thaw action.

specimens are fully dried in the air before the tests, screened by 2mm, prepared with different water contents, and stored in self-sealed bags for at least 48h for standby.

3.2 Methods

3.2.1 Soil specimen preparation

The soil specimens are prepared into cylinders, whose both ends are flat and kept perpendicular to the long axis. The dry densities for mechanical and permeability test are 1.58g/cm³, 1.69g/cm³ and 1.80g/cm³, the water contents are 10.0%, 13.3% and 16.6%. Their diameters and heights are 39.1 mm and 80 mm for mechanical specimen size, and 61.8mm and 40mm for permeability test. The dry densities of the specimens for heat conduction test are 1.50g/cm³, 1.58g/cm³, 1.69g/cm³, 1.80g/cm³ and 1.90g/cm³, the water contents are 6.0%, 10.0%, 13.3%, 16.6% and 20.0%, respectively, and their sizes are same with those of permeability specimens.

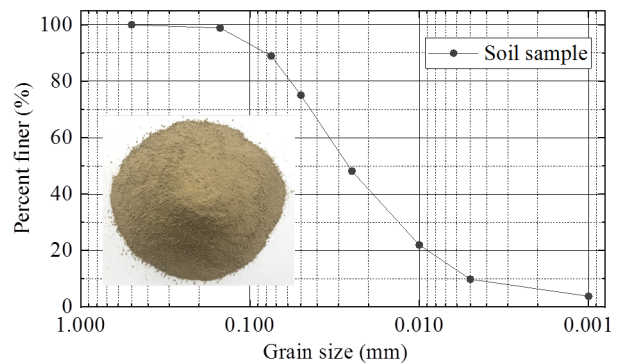
3.2.2 Freeze-thaw test

After preparation, each soil specimen shall be tightly wrapped immediately with a preservative film to prevent water loss or immersion. According to the research results of Hu Tianfei and Chang Dan et al. (Chang et al 2014; Hu et al 2017), the disturbance of



Fig. 3 Location of the study area of Liugou Reservoir area at the northern foot of Tianshan Mountain. (a) Map of the Xinjiang Uygur Autonomous Region. (b) The top view of the reservoir. (c) The top view of the soil bank slope. (d) The real view of the soil bank slope. (e) The real view of the local bank slope collapse.

soil specimens freezing at -15°C is the largest, and they can be completely frozen within 12h. The experimental cooling temperature of -15°C is within the range of winter temperature variation at the northern foot of Tianshan Mountain, and it is close to the average temperature (-18°C) of the coldest month, which is in line with the engineering practice. To ensure that the soil specimens can be completely frozen and thawed, they are put into a low-temperature box of -15°C , freezing for 24 hours, and then placed in a room temperature environment at about 20°C to melt for 24 hours to complete a freeze-thaw cycle. The existing research results indicate that the soil specimens attain dynamic equilibrium after 3-7 freeze-thaw cycles, their failure strength values reaches the lowest points, and the values have little change with the increasing freeze-thaw cycles on the basis (Ishikawa and Miura 2011; Liu et al. 2016; Tang et al. 2017). Therefore, the freeze-thaw cycles of 0, 1, 3, 5 and 7 were carried out to test the soil properties.



which can reflect the soil mechanical properties (Liu et al. 2020b). These two parameters are used to evaluate the effect of freeze-thaw cycles on the soil mechanical properties. The consolidated undrained (CU) triaxial tests are conducted on the specimens after different freeze-thaw cycles using the GDS triaxial test system. The confining pressures are taken as 50kPa, 100kPa, 200kPa and 300kPa, respectively, according to the height of the bank slope. The specimens are fully saturated before the test and wrapped with rubber films to isolate them from the external water during the test. The strain shear rate is set to 0.5%/min.

3.2.4 Permeability test

A permeameter (TST-55) is used to carry out the falling-head permeation test according to the "Specification of soil test" (Ministry of Water Resources of the People's Republic of China 2019), and the permeability coefficients of the specimens after the freeze-thaw cycles was obtained.

3.2.5 Heat conduction test

The thermal characteristic analyzer (ISOMET-2104) is utilized to test the specimens. Its test range is 0.2~6.0W/(m·K) (two probes available) with an accuracy of $\pm 5\%$, and the applicable temperature range is $-15\sim 50^\circ\text{C}$. It is based on transient probe technique to measure the temperature response of the material to the heat flow pulse, so that the resistance heater inserted in the probe generates heat flow, which makes the probe directly contact with the sample to be tested (Aggarwal et al 2009). The thermal conductivity is obtained by the change of sample temperature with time in a certain time interval. The calculation formula of thermal conductivity is given by (Milena et al 2019):

$$\lambda_T = -\frac{q_T}{\text{grad}T} \quad (1)$$

where λ_T is thermal conductivity, W/(m·K); q_T is heat flow density vector, W/m²; T is temperature, °C.

4 Results and Analyses

4.1 Effect of freeze-thaw cycles on mechanical properties

4.1.1 Stress-strain relationship after freeze-thaw cycles

The relationship curves between the deviator

stress ($q = \sigma'_1 - \sigma'_3$) and the axial strain (ϵ) of the soil specimens with different water contents and dry densities under different freeze-thaw cycles are drawn according to the above-mentioned triaxial test results, as shown in Fig. 5. The data before "-" in the legend shows the number of freeze-thaw cycles, and that after "-" shows the confining pressure applied during the triaxial test.

It can be seen from Fig.5 that the stress-strain curves are mainly affected by the dry densities, water contents, freeze-thaw cycles and confining pressures. They show the softening characteristics of the stress-strain curves weaken in general with the increase of the freeze-thaw cycles, dry densities and water contents. For the specimens with a high dry density (1.80 g/cm³), the softening characteristics of the curves are prominent, and there is a peak value. The stress-strain curve characteristics of the medium density (1.69g/cm³) soil specimens are between them. The ice crystals expand and compress the surrounding soil particles when the water freezes into ice in the cold environment. When the soil melts, the pores produced by some ice crystal expansion cannot be completely restored to the original state, so as to increase the pore volumes of the specimens, change the arrangement of the soil particles, and reduce their connection forces (Taina et al. 2013; Zhou et al. 2019). When the specimens with low water contents are frozen, the ice crystal content is small, the expansion degree of the soil is a little, the volume size and quantity of pores formed after melting are small as well, and the influence level of the freezing and thawing process is relatively low. The large confining pressures will reduce the pore volumes increased by the freezing and thawing processes, and the soil strength can be restored to a larger extent (Chen et al. 2018). Therefore, the increase of freeze-thaw cycles has a significant impact on the stress-strain curves of the specimens under low and medium confining pressures (100kPa and 50kPa) with high water contents (13.3% and 16.6%), and has no obvious influence on that of the specimens with a low water content (10.0%) and high confining pressures (200kPa and 300kPa). Some research results indicate that the type of stress-strain curves is not affected by the freeze-thaw cycles due to the different test conditions and materials (Vahdani et al. 2020).

It is found that the relationship between the stress-strain curves and the failure modes of the specimens are much closer. The failure modes of the

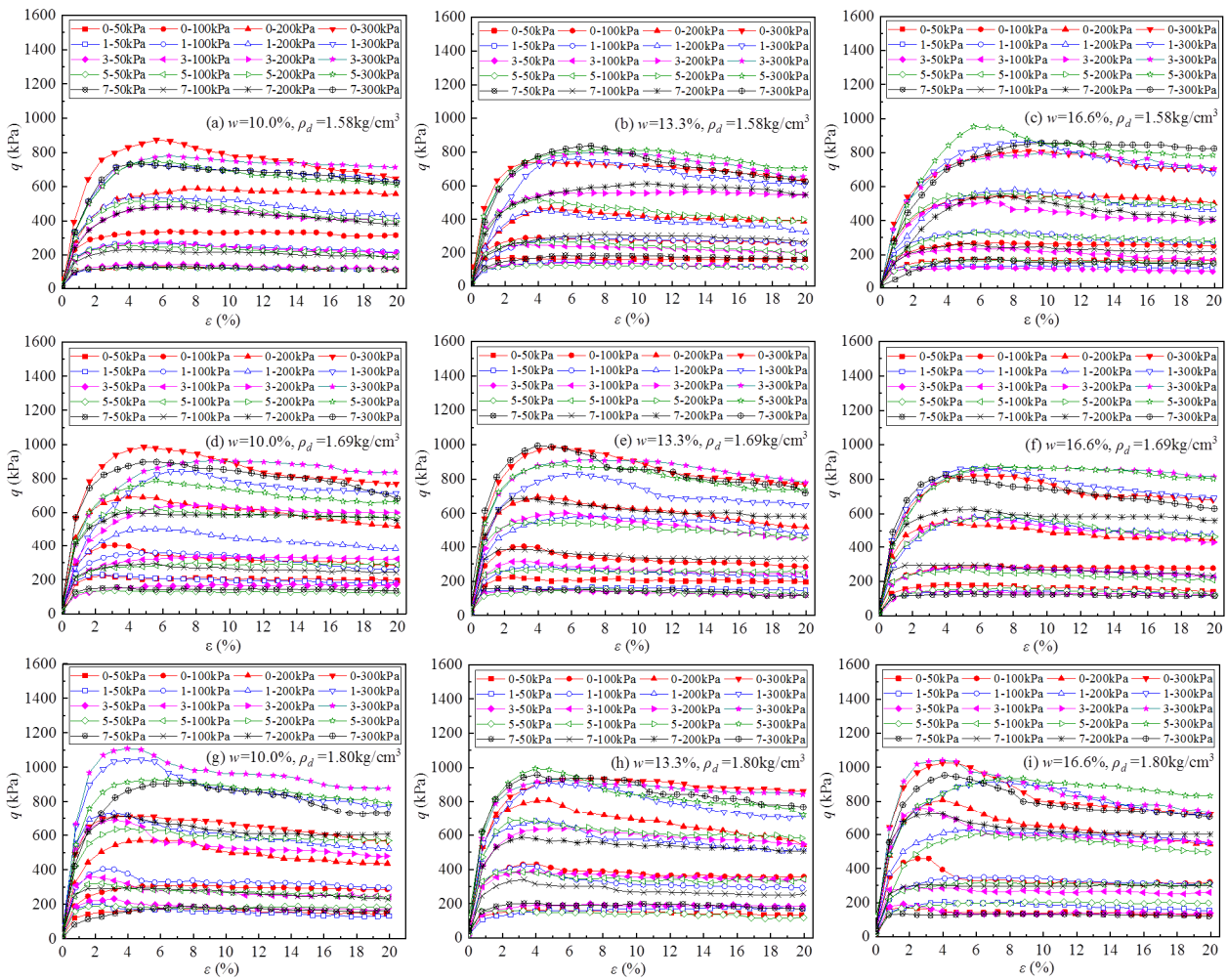


Fig. 5 The stress-strain curves of the soil specimens from the selected research section of Liugou Reservoir with different water contents (w) and dry densities (ρ_d) under freeze-thaw cycles. (q , deviator stress; ε , he axial strain.)

specimens with different dry densities are quite different, as shown in Fig. 6. The difference is shown in the stress-strain curves. The high dry density (1.80 og/cm^3) specimens show obvious shear planes after failure, as shown in Fig.6a. Their stress-strain curves gradually decreased after reaching the highest points, showing obvious softening characteristics. The shear plane is not obvious when their dry density is reduced to 1.69 g/cm^3 , and the bulge appears in the middle of the specimens, as shown in Fig.6b. The decreasing range of them is slower than that of high dry density specimens when the curves reach the highest points, and their softening characteristics are weakened. For the low dry density (1.58 g/cm^3) specimens, no shear plane is found after loading, and the obvious bulge appeared in the middle, as shown in Fig.6c. Their stress-strain curves are almost horizontal straight lines at low confining pressures

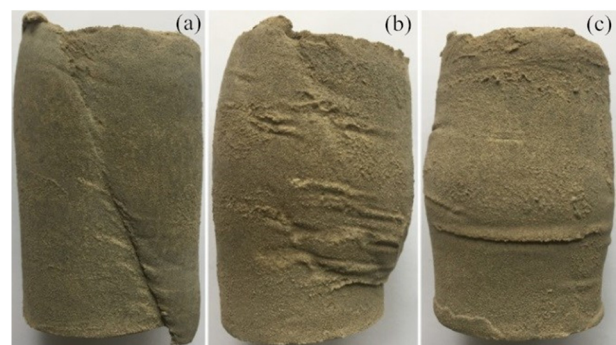


Fig. 6 Typical failure modes of the specimens with different densities from the selected research section of Liugou Reservoir. (a) 1.80 g/cm^3 , (b) 1.69 g/cm^3 , (c) 1.58 g/cm^3 .

(50kPa, 100kPa) after rising to the highest points, and the decrease range at high confining pressures (200kPa, 300kPa) is relatively gentle, showing hardening characteristics.

4.1.2 Effect on the cohesions and internal friction angles

4.1.2.1 Changes of the effective cohesions

The relationship between the effective cohesions (c') of the specimens and the number of freeze-thaw cycles (N_T) under different dry densities and water contents is shown in Fig. 7.

It can be seen from Fig.7 that the initial water contents of the specimens has a certain influence on their effective cohesions. The effective cohesions decrease with the increasing initial water contents in general. In the preparation of soil specimens, it is found that the soil particles are easy to disperse when the water content is low, and the particle distribution is relatively uniform. When it is increased, the fine particles have aggregation effect, and large holes are easy to appear in the specimens. The uniform degree of the pore distribution reduces and the internal defects are increased, which makes the strength of the specimens with high initial water contents lower. Ye et al. (2019) believe that the cohesions are sensitive to the change of the initial water contents, and their triaxial test results also have similar laws. The effective cohesions decrease after freeze-thaw, and the maximum drop is after the first freeze-thaw cycle. The decrease range of the effective cohesions gradually abates after 3-5 freeze-thaw cycles. Their values decrease with the increase of the water contents under the same dry densities, and the larger the dry densities are, the more significant the influence of the water content changes on the effective cohesions is. The effective cohesions are raised with the increasing dry densities under the same water contents, and the larger the dry densities are, the more obvious their reduction is. The curves of the effective cohesions and freeze-thaw cycles are fitted to accurately predict the effect of freeze-thaw cycles on the soil mechanical properties. The results show that their change laws obey the exponential function, and the expression is given by:

$$c' = b + ae^{-N_T/\lambda} \tag{2}$$

where c' is the effective cohesion, kPa; N_T is the number of freeze-thaw cycles; a , b and λ are fitting parameters, whose values are related to the dry density, water content and the number of freeze-thaw cycles, as shown in Table 1.

4.1.2.2 Changes of the effective internal friction angles

The relationship curves between the effective

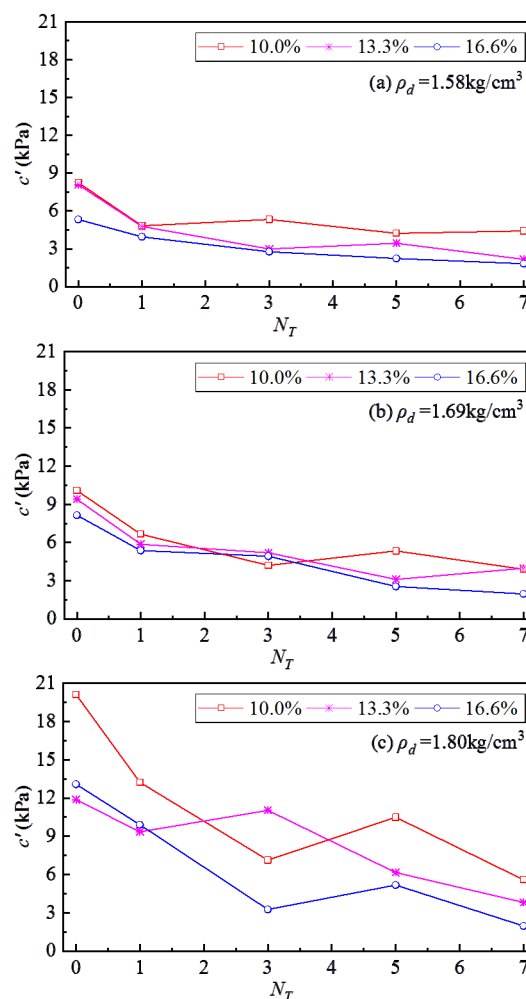


Fig. 7 The change law of the effective cohesions (c') of the specimens and the number of freeze-thaw cycles (N_T) under different dry densities and water contents.

Table 1 The parameter values of the fitting formulas

Test groups	a	b	λ	R^2
$\rho_d=1.58 \text{ g/cm}^3$, $w=10.0\%$	3.5914	4.6585	0.3251	0.9360
$\rho_d=1.58 \text{ g/cm}^3$, $w=13.3\%$	5.3306	2.7378	1.0552	0.9644
$\rho_d=1.58 \text{ g/cm}^3$, $w=16.6\%$	3.5599	1.7157	2.3674	0.9965
$\rho_d=1.69 \text{ g/cm}^3$, $w=10.0\%$	5.7121	4.3958	1.0124	0.9470
$\rho_d=1.69 \text{ g/cm}^3$, $w=13.3\%$	5.5060	3.7832	1.2511	0.9305
$\rho_d=1.69 \text{ g/cm}^3$, $w=16.6\%$	7.1985	0.5367	4.3427	0.9337
$\rho_d=1.80 \text{ g/cm}^3$, $w=10.0\%$	12.7944	7.3909	1.1935	0.8970
$\rho_d=1.80 \text{ g/cm}^3$, $w=13.3\%$	-1.9716	13.2752	-4.3997	0.8658
$\rho_d=1.80 \text{ g/cm}^3$, $w=16.6\%$	10.9526	2.3888	2.0303	0.9154

Note: w , water contents; ρ_d , dry densities.

internal friction angles of the specimens and the freeze-thaw cycles under different dry densities and water contents are shown in Fig. 8.

It can be seen from Fig.8 that the effective internal friction angles of the specimens have an increasing trend in general with the increasing freeze-thaw cycles, but the change process fluctuates memorably and the change laws are not obvious. The effective internal friction angles rise with the increasing dry densities under the same water contents. The relationship between the effective internal friction angles and the water contents is irregular under the same dry densities. The essence of the internal friction angles is to reflect the contact and occlusion between particles in the failure process. The arrangement of the soil particles and the size of the adhesion areas between particles will affect their values (Yao et al. 2017). The process of freeze-thaw cycles is accompanied by the water migration and the phase transformation between water and ice, which has a certain disturbance on the specimens, especially in the first freeze-thaw cycle, and the fluctuation of their effective internal friction angles is generally large. However, the contact and arrangement of the soil particles are very random. The freeze-thaw effect changes the relative position between them and the internal micro structure of the specimens. The arrangement of the particles after the change is still random, resulting in that the change law between the internal friction angles and the freeze-thaw cycles is not obvious. The effect of freeze-thaw cycles on the internal friction angles is very controversial at present, and the results obtained by different types of soil specimens and different researchers are quite discrepant (Han et al. 2018; Tang et al. 2018; Wang et al. 2018; Zhang et al. 2020; Zhang et al. 2019), which need further study.

4.2 Effect of freeze-thaw cycles on permeability coefficients

The relationship curves between the permeability coefficients of the specimens and the freeze-thaw cycles under different dry densities and water contents are shown in Fig. 9.

It can be seen from Fig. 9 that the permeability coefficients of the specimens before freeze-thaw cycles are greatly affected by initial water contents. They enlarge with the increasing initial water contents under the same dry densities. That may be caused by

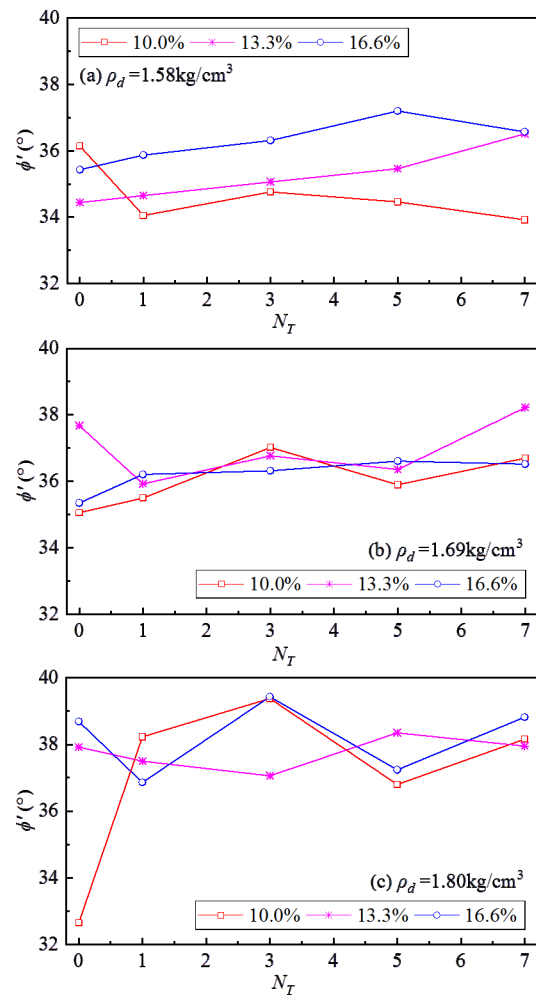


Fig. 8 The relationship curves between the effective internal friction angles (ϕ') of the soil specimens and the freeze-thaw cycles (N_T) under different water contents (w) and dry densities (ρ_d).

the agglomeration effect of the fine particles during the high water content specimen preparation, which increases the seepage flow channels in the soil. The permeability coefficients of the specimens under the same water contents decrease with the increase of dry densities, which are consistent with the actual situation of the projects. They are raised with the increase of freeze-thaw cycles, and the first freeze-thaw cycle has the significant impact on them. The permeability coefficients of the low dry density (1.58 g/cm^3) specimens decrease first and then enlarge with the increase of freeze-thaw cycles. For the medium and high dry densities (1.69 g/cm^3 and 1.80 g/cm^3), they increase with the increasing freeze-thaw cycles. The low dry density specimens are more significantly affected by the freeze-thaw cycles, and their permeability coefficients fluctuate evidently. The

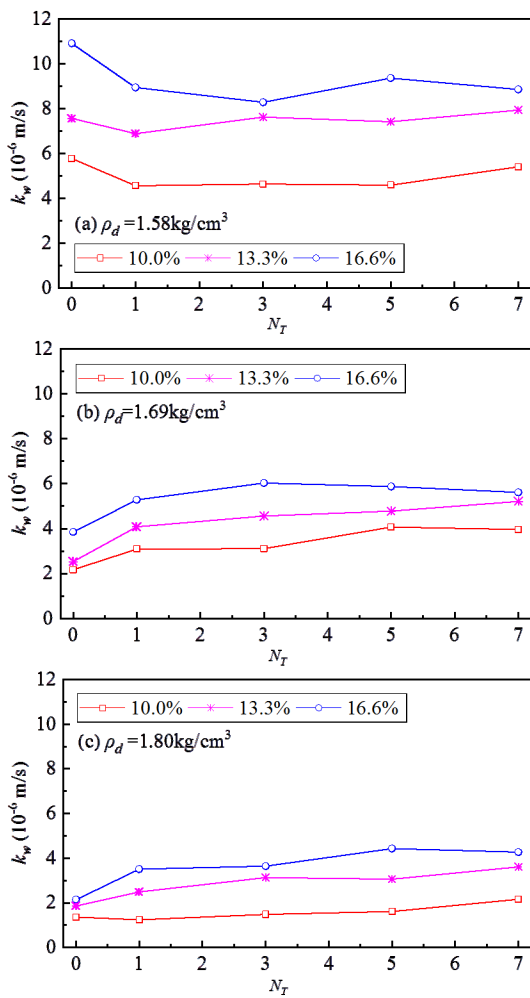


Fig. 9 The relationship curves between the permeability coefficients (k_w) of the soil specimens and the freeze-thaw cycles (N_T) under different water contents (w) and dry densities (ρ_d).

freezing and thawing processes increase the pore volume and the connectivity between pores, and then enlarges the permeability coefficients (Lu et al. 2019; Zhang and Cui 2018). The high-density specimens are relatively dense inside, and the water migration is relatively slow. The soil particles have a certain constraint on the expansion of ice crystal bodies, and the arrangement between the soil particles is more compact. The internal pore volume is relatively small, and it is difficult to connect these pores through the freeze-thaw effect, thus the permeability coefficients of the high-density specimens are less affected by freeze-thaw cycles.

4.3 Effect of freeze-thaw cycles on thermal properties

The thermal conductivities are dramatically

affected by the water content and dry density of the soil specimens. It is necessary to discuss their effect on the thermal conductivities before analyzing the effect of freeze-thaw cycles on them. The relationship curves of the thermal conductivities with the dry densities and water contents are shown in Fig. 10. The water contents of the air dried soil specimens with the dry densities of 1.50g/cm³, 1.58g/cm³, 1.69g/cm³, 1.80g/cm³ and 1.90g/cm³ are 2.3%, 2.6%, 2.7%, 3.1% and 3.3%, respectively.

It can be seen from Fig.10a that the thermal conductivities of the specimens under the same water contents enlarge gradually with the increase of the dry densities, and the relationship between them is almost linear. As shown in Fig.10b, the thermal conductivities of the specimens increase nonlinearly with the increasing water contents. These are consistent with the general laws of the remolded soil specimens (Hu et al. 2017; Zhen et al. 2019).

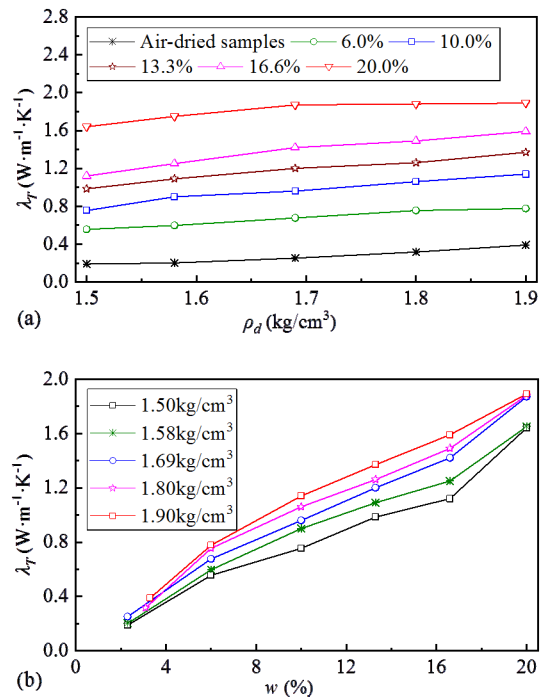


Fig. 10 The effect of the dry densities (ρ_d) (a) and water contents (w) (b) on the thermal conductivities (λ_T) of the soil specimens.

The relationship curves between the thermal conductivities of the specimens and the freeze-thaw cycles under different water contents and dry densities are shown in Fig. 11.

It can be seen from Fig.11 that the thermal conductivities of the specimens under the same water contents decrease with the increase of the freeze-thaw

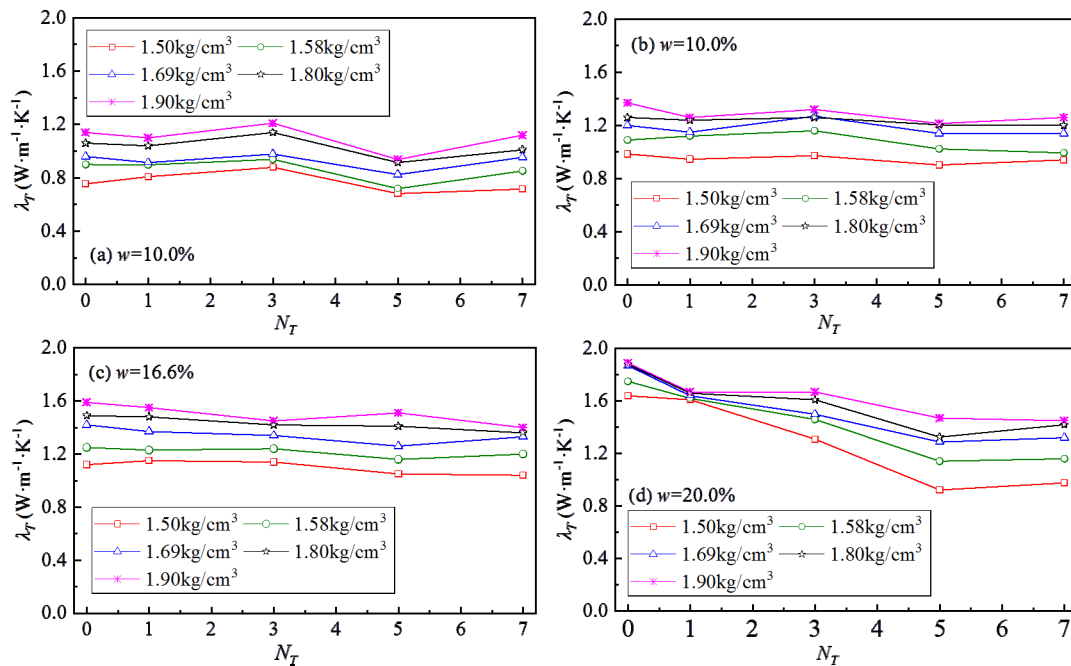


Fig. 11 The effect of freeze-thaw cycles (N_T) on the thermal conductivities (λ_T) of the soil specimens. (a) $w=10.0\%$. (b) $w=13.3\%$. (c) $w=16.6\%$. (d) $w=20.0\%$

cycles. When the water contents are less than or equal to 16.6%, the degree of phase transition between ice and water is relatively low and the soil pore structure changes little, the thermal conductivities descend slowly with the freeze-thaw cycles and the effect on them is not significant. When the water content increases to 20.0%, the freeze-thaw effect on them increases markedly, especially for the specimens with low dry densities (1.50g/cm³, 1.58g/cm³ and 1.69g/cm³), their thermal conductivities decrease evidently. The effect of freeze-thaw cycles on high dry density (1.80g/cm³ and 1.90g/cm³) specimens is relatively little. Their thermal conductivities are not only affected by the temperature variations and water contents, but also related to their micro structures (Rui et al. 2019). The soil volume change, the grain size distribution and the crack formation all have a significant influence on the thermal conductivities in the freeze-thaw process (Moghbel and Fall 2018). The pore volumes of the specimens with low densities and high water contents are large under the same water contents compared with the high dry density ones, the arrangement of the particles is more irregular and their saturation is low as well. The pores between the soil particles are easy to connect after freeze-thaw cycles, the thermal resistance becomes larger, and the thermal conductivities are significantly reduced. However, for different soil types and testing environments, the main influencing factors and

change laws of the thermal conductivities after freeze-thaw cycles are quite discrepant (Overduin et al. 2006; He et al. 2018), which needs further study.

4.4 Changes of the micro structures

The soil specimens with dry density of 1.69g/cm³ are selected for electron microscope scanning to understand their micro structures before and after freeze-thaw cycles. The influence of the initial water contents on the micro structures and the change characteristics of the soil particles are observed after the specimen micro structures are magnified 100 times, 500 times and 5000 times, as shown in Fig. 12.

It can be seen from Fig. 12a and b that the specimens with high initial water contents have more obvious agglomeration effect of the soil particles, worse distribution uniformity of the particles, and higher probability of large pores with the same dry densities, which is more obvious on the specimens with high water contents and low dry densities. For the specimens with low water contents, the arrangement of the soil particles is more regular and the distribution of the pores is more uniform. These differences have a remarkable influence on the internal friction angles and permeability coefficients. The soil particle surfaces are relatively smooth before freeze-thaw cycles, and there are less fine matters around, as shown in Fig. 12c and e. However,

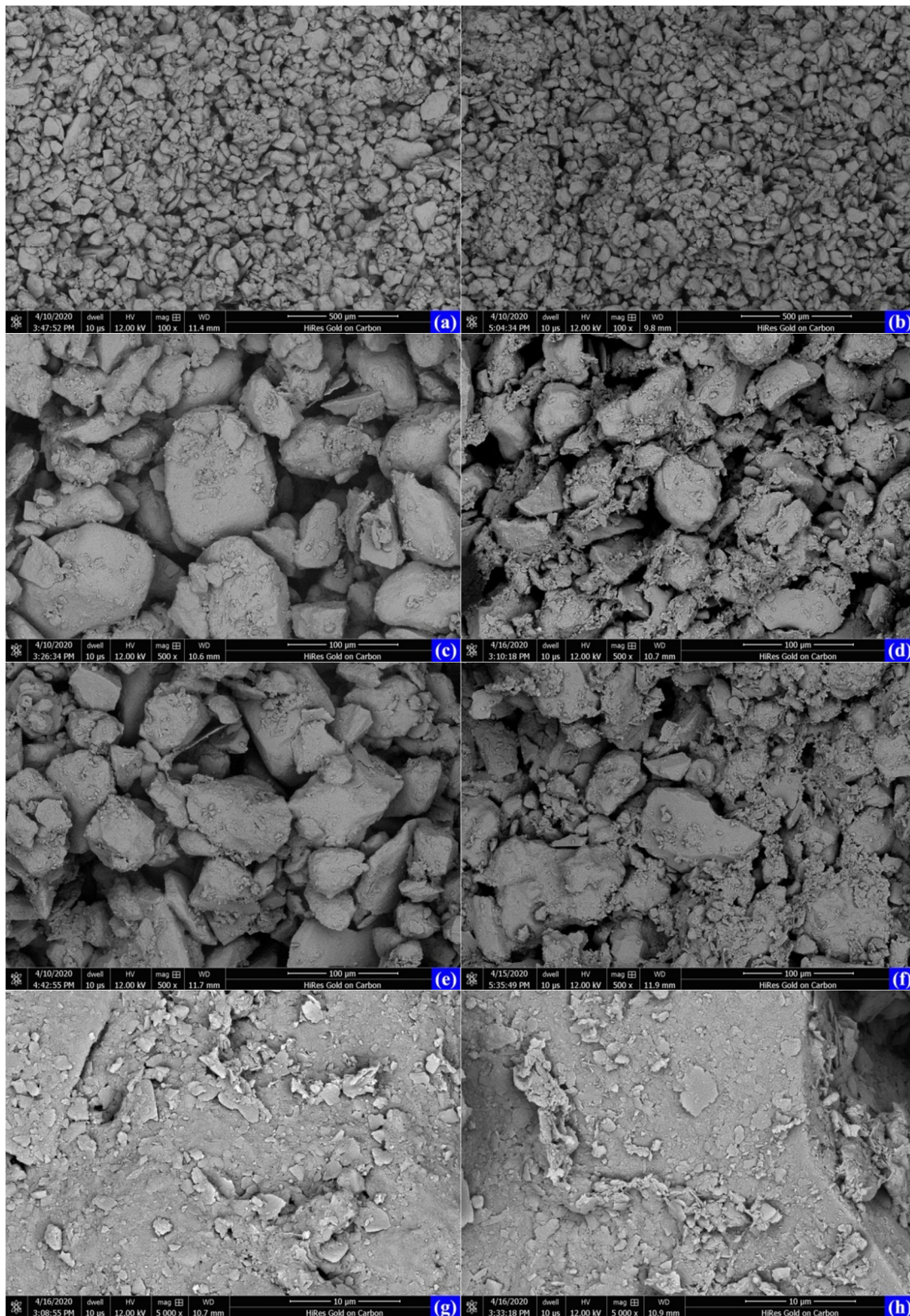


Fig. 12 The scanning electron micrographs of the soil specimens. (a) The soil specimens without freeze-thaw cycles (magnified by 100 times), $w=10.0\%$. (b) The soil specimens without freeze-thaw cycles (magnified by 100 times), $w=20.0\%$. (c) The soil specimens without freeze-thaw cycles (magnified by 500 times), $w=13.3\%$. (d) The soil specimens (magnified by 500 times) after 7 freeze-thaw cycles, $w=13.3\%$. (e) The soil specimens without freeze-thaw cycles (magnified by 500 times), $w=16.6\%$. (f) The soil specimens (magnified by 500 times) after 7 freeze-thaw cycles, $w=16.6\%$. (g) The soil specimens (magnified by 5000 times) after 7 freeze-thaw cycles, $w=13.3\%$. (h) The soil specimens (magnified by 5000 times) after 7 freeze-thaw cycles, $w=16.6\%$.

a large number of sheet structures are adhered on the surfaces and around the soil particles after 7 freeze-thaw cycles, as shown in Fig.12d and f. When the particles are further magnified by 5000 times, it can be seen that these flake structures are formed on and around their surfaces after peeling off from the soil particles in the freeze-thaw processes. It is not obvious after the first and third freeze-thaw cycles, but became more significant after the seventh freeze-thaw cycle. It can be predicted that the phenomenon will become more obvious with the increase of freeze-thaw cycles. That indicates the long-term freeze-thaw cycles can break the soil particles, change the soil micro structures, produce more fine flaky particles, and cause the rearrangement of the soil particles. These micro changes are reflected in the variations of the soil engineering characteristics (Zhang et al. 2019).

4.5 Mechanism analyses of the freeze-thaw damage

The specimens are tightly wrapped all the time with fresh-keeping films in the freezing and thawing processes, thus they are all in a closed environment and cannot exchange materials with the outside. The freezing temperature is -15°C , and the melting temperature is about 20°C (the room temperature). The surfaces of the specimens freeze first when they are freezing at the constant temperature environment. A temperature gradient is formed between their surfaces and internal unfrozen areas, which make the water to migrate from the unfrozen areas to the freezing fronts, and the ice crystals are precipitated on the specimen surfaces, as shown in Fig.13.

It can be seen from Fig.13 that the higher the water contents are, the more ice crystals precipitate on the specimen surfaces during the freezing process. The water migration will further increase the water contents of the surface soil (Li et al. 2017), and it is easy to make the surface soil reach or close to the saturated state when the initial water content of the specimens is high. The water in the surface soil freezes to form ice crystals when the temperature drops to the freezing temperature. The ice crystals expand in volume, which enlarge the distance between the soil particles, and disturb the arrangement and distribution of the particles (Wei et al. 2019). The temperature gradient disappears and the water migration ends when the temperature of the whole specimen is constant at -15°C . The surface soil

temperature rises first and starts to melt when they are taken out from the low temperature box and placed in the room temperature environment for melting. At this time, the temperature in the middle parts is lower than that of the specimen surfaces, and the temperature gradient is formed again in the soil. The water begins to move from the surfaces to the middle parts of the non-melting areas until the temperature gradient disappears. The water migration process cannot be completely reversible due to the gravity effect, and the water content is different in the direction perpendicular to the freezing surface of the specimens (Steiner et al. 2018). The amount of water migrated from the center of the specimens to the surface in the freezing process is larger than that of the water migration to the opposite direction during the melting process (Wang et al. 2005). The ice crystals all change into water when they melt completely, and the volumes expanded from the ice crystals shrink, and the specimen volumes also decrease under the action of self-weight. They amplified by water freezing expansion cannot be completely recovered because the soil is an elastic plastic material and its elastic range is very small (Xie et al. 2015). In this way, there are a large number of pores left after it melted, which makes the pore volumes in the specimens increase compared with that before freezing (Zhang and Cui 2017). For the

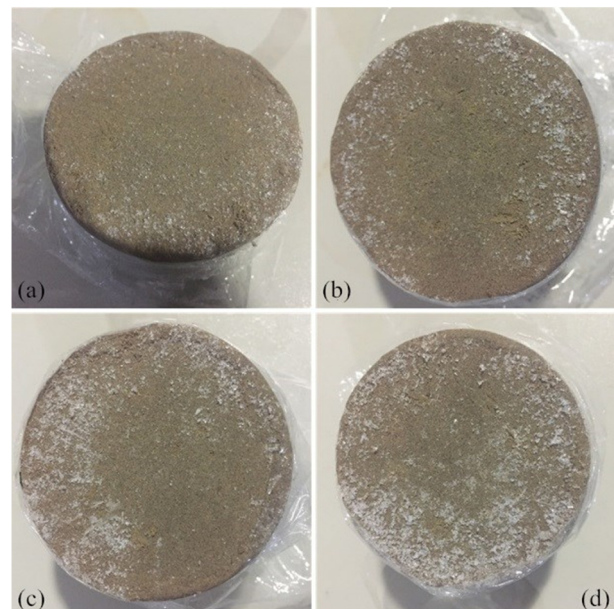


Fig. 13 The ice crystals precipitated on the surfaces of the specimens with the dry density of 1.69 g/cm^3 under different water contents during the freezing process. (a) $w=10.0\%$. (b) $w=13.3\%$. (c) $w=16.6\%$. (d) $w=20.0\%$

high water content specimens, the phenomenon is more significant because of the violent water migration (Ding et al. 2019). The micro cracks will be formed if there are connections between pores, which will cause the damage to the specimens (Xu et al. 2019). The effect of freeze-thaw cycles in the processes is irreversible (Liu et al. 2019). The existence of the pores and micro-cracks will reduce the soil mechanical properties and increase the permeability. The thermal conductivities of the high water content specimens decrease substantially after freeze-thaw cycles because the thermal conductivity of the air is smaller than that of the soil particles and the porosity of the high water content specimens increases greatly. There are many pores in the low density (1.50g/cm³, 1.58g/cm³ and 1.69g/cm³) soil. In the case of high water contents (16.6% and 20.0%), the water migration and the phase transformation between water and ice is more intense, which is easy to connect these existing pores. Therefore, the specimens with low dry densities and high water contents are generally affected significantly by freeze-thaw cycles. The volume changes and water migration of the specimens reach a relative equilibrium state after 3-5 freeze-thaw cycles, and their mechanics, permeability and heat conduction tend to be stable.

The above analyses indicate that the water migration and the phase transformation between water and ice are the main factors affecting the soil engineering properties during the freezing-thawing processes. The processes in the above indoor tests are all conducted in a closed environment, and there is no external water supply. However, the soil freezing and thawing in the actual projects is carried out in an open system. The soil in the middle and lower parts of the reservoir soil bank slopes in cold regions will cause violent water migration after freezing under the condition of abundant external water supply (Lu et al. 2019; Wang et al. 2019). The higher the initial water content is, the more vigorous the water migration in the soil is in the freezing process (Wang et al. 2015). Therefore, the soil there is most seriously damaged by freeze-thaw cycles, as shown in Fig.1d. At the beginning and end of winter, the temperature difference between day and night at the northern foot of Tianshan Mountain is large, and the ice water phase changes will cause a large number of pores and micro cracks in the soil surfaces. These pores will be further connected to form micro cracks with the process of water migration and ice water phase

changes caused by multiple freeze-thaw cycles, and the existing micro cracks will also expand (Tang et al. 2018). In the open environment, the soil freezing and thawing processes are very different from that in the closed system (Lu et al. 2019). The volume changes and water transfer of the soil are more intense during freezing and thawing, and it is difficult to achieve the dynamic equilibrium (Xian et al. 2019). In addition, the long-term freeze-thaw cycles have a crushing effect on the soil particles. Therefore, the soil engineering characteristics will continue to change with the increasing freeze-thaw cycles, and the easily observed phenomenon is that the cracks on the soil surfaces are increasing, widening and extending, as shown in Fig.1(b), (c) and (d) and Fig. 2. The soil blocks of the bank slopes will fall or collapse when these cracks penetrate, as shown in Fig.1e.

5 Conclusions

Based on a large number of field investigations on dozens of reservoir soil bank slopes at the northern foot of Tianshan Mountain, laboratory tests were carried out to quantitatively analyze the effect of freeze-thaw cycles on the soil engineering characteristics of the mechanics, permeability and heat conduction, and to reveal the promotion of freeze-thaw cycles on their failure. The following main conclusions are made:

(1) The softening characteristics of the stress-strain curves weaken in general with the increasing freeze-thaw cycles, and it is more obvious under low dry densities and low confining pressures. The stress-strain curves are closely related to the failure modes of the specimens. The effective cohesions decrease exponentially with the increase of freeze-thaw cycles, and the change laws of the effective internal friction angles with freeze-thaw cycles are not obvious.

(2) The permeability coefficients of the unfrozen specimens are affected by the initial water contents, and enlarge with their increase. They increase with the increase of freeze-thaw cycles in general, and those of the specimens with low dry densities fluctuate significantly.

(3) The thermal conductivities are raised with the increase of dry densities and water contents and decrease with the increasing freeze-thaw cycles. The freeze-thaw effect on the thermal conductivities is not significant when the water contents are low. The effect increases appreciably when the specimens are

nearly saturated. Those of the specimens with low dry densities and high water contents decrease substantially after the freeze-thaw cycles.

(4) The water migration and ice water phase changes result in the variations of soil internal structures in the freezing-thawing processes, which is the main factor that causes the changes of the soil engineering characteristics. In an open environment

in cold regions, the sufficient water supply and the alternation of positive and negative temperatures make the water transfer and ice water phase changes in the soil very intense, and the soil volume changes and the water transfer are difficult to reach a balance. It is easy to form a large number of pores and micro cracks in the soil freezing-thawing areas. The soil on the bank slopes will fall or collapse when these cracks penetrate.

Acknowledgments

The authors wish to express their gratitude to Dr. ZHANG Shujuan, Dr. YANG Chengsong and Dr. HE Rui-xia for their help in the experiments. This research was supported by the National Key Research and Development Program of China (Grant No. 2018YFC0809605, 2018YFC0809600), the Key Research Program of Frontier Sciences of Chinese

Academy of Sciences (Grant No. QYZDY-SSW-DQCo15), the National Natural Science Foundation of China (Grant No. 41230630), the National Science Fund for Distinguished Young Scholars (Grant No. 41825015), the Key Research Program of the Chinese Academy of Sciences (Grant No. ZDRW-ZS-2020-1).

References

- Aggarwal RK, Negi PS, Satyawali PK (2009) New density-based thermal conductivity equation for snow. *Defence Sci J* 59(2): 126-130.
<https://doi.org/10.14429/dsj.59.1499>
- Benson CH, Abichou TH, Olson MA, et al. (1995) Winter effects on hydraulic conductivity of compacted clay. *J Geotech Eng-ASCE* 121(1): 69-79.
[https://doi.org/10.1061/\(ASCE\)0733-9410\(1995\)121:1\(69\)](https://doi.org/10.1061/(ASCE)0733-9410(1995)121:1(69))
- Chang D, Liu JK, Li X, et al. (2014) Experiment study of effects of freezing-thawing cycles on mechanical properties of qinghat-tibet silty sand. *Chin J Rock Mech Eng* 33(7): 1496-1502. (In Chinese)
<https://doi.org/10.13722/j.cnki.jrme.2014.07.023>
- Chen H, Zhu Z, Wang Z (2020) Constitutive model with double yield surfaces of freeze-thaw soil considering moisture migration. *Bul Eng Geol Environ* 79(5): 2353-2365.
<https://doi.org/10.1007/s10064-019-01673-1>
- Chen J, Xie X, Zheng X, et al. (2020) Effects of sand-mulch thickness on soil evaporation during the freeze-thaw period. *Hydrol Process* 34(13): 2830-2842.
<https://doi.org/10.1002/hyp.13766>
- Chen L, Chen Z, Jia G, et al. (2020) Influences of forest cover on soil freeze-thaw dynamics and greenhouse gas emissions through the regulation of snow regimes: A comparison study of the farmland and forest plantation. *Sci Total Environ* 726: 138403.
<https://doi.org/10.1016/j.scitotenv.2020.138403>
- Chen S, Kong L, Xu G (2018) An effective way to estimate the Poisson's ratio of silty clay in seasonal frozen regions. *Cold Reg Sci Technol* 154: 74-84.
<https://doi.org/10.1016/j.coldregions.2018.06.003>
- Dalla Santa G, Cola S, Secco M, et al. (2019) Multiscale analysis of freeze-thaw effects induced by ground heat exchangers on permeability of silty clays. *Geotechnique* 69(2): 95-105.
<https://doi.org/10.1680/jgeot.16.P.313>
- Ding Z, Kong B, Wei X, et al. (2019) Laboratory testing to research the micro-structure and dynamic characteristics of frozen-thawed marine soft soil. *J Mar Sci Eng* 7(4): UNSP 85.
<https://doi.org/10.3390/jmse7040085>
- Du L, Dyck M, Shotyky W, et al. (2020) Lead immobilization processes in soils subjected to freeze-thaw cycles. *Ecotox Environ Safe* 192: 110288.
<https://doi.org/10.1016/j.ecoenv.2020.110288>
- Han Y, Wang Q, Wang N, et al. (2018) Effect of freeze-thaw cycles on shear strength of saline soil. *Cold Reg Sci Technol* 154: 42-53.
<https://doi.org/10.1016/j.coldregions.2018.06.002>
- He RX, Jin HJ, Zhao SP, et al. (2018) Review of status and progress of the study in thermal conductivity of frozen soil. *J Glaciol Geocry* 40(1): 116-126. (In Chinese)
<https://doi.org/10.7522/j.issn.1000-0240.2017.0314>
- Hou R, Li T, Fu Q, et al. (2020) The effect on soil nitrogen mineralization resulting from biochar and straw regulation in seasonally frozen agricultural ecosystem. *J Clean Prod* 255: 120302.
<https://doi.org/10.1016/j.jclepro.2020.120302>
- Hu G, Zhao L, Wu X, et al. (2017) Comparison of the thermal conductivity parameterizations for a freeze-thaw algorithm with a multi-layered soil in permafrost regions. *Catena* 156: 244-251.
<https://doi.org/10.1016/j.catena.2017.04.011>
- Hu TF, Liu JK, Fang JH, et al. (2017) Experimental study on the effect of cyclic freezing-thawing on mechanical properties of silty clay under different cooling temperatures. *Chin J Rock Mech Eng* 36(7): 1757-1767. (In Chinese)
<https://doi.org/10.13722/j.cnki.jrme.2016.1576>
- Ishikawa T, Miura S (2011) Influence of freeze-thaw action on deformation-strength characteristics and particle crushability of volcanic coarse-grained soils. *Soils Found* 51(5): 785-799.
<https://doi.org/10.3208/sandf.51.785>
- Kawamura S, Miura S (2013) Rainfall-induced failures of volcanic slopes subjected to freezing and thawing. *Soils Found* 53(3): 443-461.
<https://doi.org/10.1016/j.sandf.2013.04.006>
- Kraatz S, Jacobs JM, Schroder R, et al. (2020) Improving SMAP freeze-thaw retrievals for pavements using effective soil temperature from GEOS-5: Evaluation against in situ road temperature data over the U.S.. *Remote Sens Environ* 237: 111545.
<https://doi.org/10.1016/j.rse.2019.111545>
- Lei H, Song Y, Qi Z, et al. (2019) Accumulative plastic strain behaviors and microscopic structural characters of artificially freeze-thaw soft clay under dynamic cyclic loading. *Cold Reg Sci Technol* 168: UNSP 102895.
<https://doi.org/10.1016/j.coldregions.2019.102895>
- Li G, Ma W, Mu Y, et al. (2017) Effects of freeze-thaw cycle on

- engineering properties of loess used as road fills in seasonally frozen ground regions, North China. *J Mt Sci* 14(2): 356-368. <https://doi.org/10.1007/s11629-016-4005-4>
- Li J, Chen N, Zhao Y, et al. (2020) A catastrophic landslide triggered debris flow in China's Yigong: factors, dynamic processes, and tendency. *Earth Surf Proc Land* 24(1): 71-82. <https://doi.org/10.15446/esrj.v24n1.78094>
- Li L, Fall M, Fang K (2020) Shear behavior at interface between compacted clay liner-geomembrane under freeze-thaw cycles. *Cold Reg Sci Technol* 172: 103006. <https://doi.org/10.1016/j.coldregions.2020.103006>
- Li R, Zhao L, Wu T, et al. (2019) Soil thermal conductivity and its influencing factors at the Tanggula permafrost region on the Qinghai-Tibet Plateau. *Agr Forest Meteorol* 264: 235-246. <https://doi.org/10.1016/j.agrformet.2018.10.011>
- Liu H, Lyu X, Wang J, et al. (2020b) The dependence between shear strength parameters and microstructure of subgrade soil in seasonal permafrost area. *Sustainability* 12(3): 1264. <https://doi.org/10.3390/su12031264>
- Liu J, Chang D, Yu Q (2016) Influence of freeze-thaw cycles on mechanical properties of a silty sand. *Eng Geol* 210: 23-32. <https://doi.org/10.1016/j.enggeo.2016.05.019>
- Liu J, Zha F, Xu L, et al. (2020) Strength and microstructure characteristics of cement-soda residue solidified/stabilized zinc contaminated soil subjected to freezing-thawing cycles. *Cold Reg Sci Technol* 172: 102992. <https://doi.org/10.1016/j.coldregions.2020.102992>
- Liu X, Liu J, Tian Y, et al. (2019) Influence of the freeze-thaw effect on the Duncan-Chang model parameter for lean clay. *Transport Geotech* 21: UNSP 100273. <https://doi.org/10.1016/j.trgeo.2019.100273>
- Liu Y, Liu E, Yin Z (2020) Constitutive model for tailing soils subjected to freeze-thaw cycles based on meso-mechanics and homogenization theory. *Acta Geotech*. <https://doi.org/10.1007/s11440-020-00937-5>
- Liu Y, Zheng W, Wang Q, et al. (2020) Evaluating sulfur-free lignin as a sustainable additive for soil improvement against frost resistance. *J Clean Prod* 251: 119504. <https://doi.org/10.1016/j.jclepro.2019.119504>
- Lu J, Wang T, Cheng W, et al. (2019) Permeability anisotropy of loess under influence of dry density and freeze-thaw cycles. *International Journal of Geomechanics* 19(9): 04019103. [https://doi.org/10.1061/\(ASCE\)GM.1943-5622.0001485](https://doi.org/10.1061/(ASCE)GM.1943-5622.0001485)
- Lu Y, Liu S, Zhang Y, et al. (2020) Freeze-thaw performance of a cement-treated expansive soil. *Cold Reg Sci Technol* 170: 102926. [https://doi.org/10.1061/\(ASCE\)GM.1943-5622.0001485](https://doi.org/10.1061/(ASCE)GM.1943-5622.0001485)
- Lu Z, She J, Wu X, et al. (2019) Cumulative strain characteristics of compacted soil under effect of freeze-thaw cycles with water supply. *Transport Geotech* 21: 100291. <https://doi.org/10.1016/j.trgeo.2019.100291>
- Lu Z, Xian S, Yao H, et al. (2019) Influence of freeze-thaw cycles in the presence of a supplementary water supply on mechanical properties of compacted soil. *Cold Reg Sci Technol* 157: 42-52. <https://doi.org/10.1016/j.coldregions.2018.09.009>
- Milena K, Marta H, Jan V, et al. (2019) Measurement of the thermal properties of innovative highly-insulating non-structural concretes. *Defect Diff Forum* 390: 41-52. <https://doi.org/10.4028/www.scientific.net/DDF.390.41>
- Ministry of Water Resources of the People's Republic of China (2019) Specification of soil test. In: SL237-2019, vol. China Water Power Press, Beijing, China. pp 120-129. (in Chinese)
- Moghbel F, Fall M (2018) Thermal properties of compost biocover subjected to freeze-thaw cycles. *Cold Regions Science and Technology* 32(3): 04018008. [https://doi.org/10.1061/\(ASCE\)CR.1943-5495.0000156](https://doi.org/10.1061/(ASCE)CR.1943-5495.0000156)
- Overduin PP, Kane DL, van Loon WKP (2006) Measuring thermal conductivity in freezing and thawing soil using the soil temperature response to heating. *Cold Reg Sci Technol* 45(1): 8-22. <https://doi.org/10.1016/j.coldregions.2005.12.003>
- Ozgul M, Aksakal EL, Gunes A, et al. (2011) Influence of global warming on aggregate stability and hydraulic conductivity under highland soil order in Turkey. *Soil Sci* 176(10): 559-566. <https://doi.org/10.1097/SS.0b013e3182288470>
- Qi J, Vermeer PA, Cheng G (2006) A review of the influence of freeze-thaw cycles on soil geotechnical properties. *Permafrost Periglac* 17(3): 245-252. <https://doi.org/10.1002/ppp.559>
- Qin Z, Lai Y, Tian Y, et al. (2019) Frost-heaving mechanical model for concrete face slabs of earthen dams in cold regions. *Cold Reg Sci Technol* 161: 91-98. <https://doi.org/10.1016/j.coldregions.2019.03.009>
- Qu Y, Chen G, Niu F, et al. (2019) Effect of freeze-thaw cycles on uniaxial mechanical properties of cohesive coarse-grained soils. *J Mt Sci* 16(9): 2159-2170. <https://doi.org/10.1007/s11629-019-5426-7>
- Qu Y, Ni W, Niu F, et al. (2020) Mechanical and electrical properties of coarse-grained soil affected by cyclic freeze-thaw in high cold regions. *J Cent South Univ* 27(3): 853-866. <https://doi.org/10.1007/s11771-020-4336-8>
- Roy D, Jia X, Steele DD, et al. (2020) Infiltration into frozen silty clay loam soil with different soil water contents in the red river of the north basin in the USA. *Water* 12(2): 321. <https://doi.org/10.3390/w12020321>
- Rui D, Zhai J, Li G, et al. (2019) Field experimental study of the characteristics of heat and water transfer during frost heaving. *Cold Reg Sci Technol* 168: UNSP 102892. <https://doi.org/10.1016/j.coldregions.2019.102892>
- Steiner A, Vardon PJ, Broere W (2018) The influence of freeze-thaw cycles on the shear strength of illite clay. *Proc Inst Civil Eng-Geotech* 171(1): 16-27. <https://doi.org/10.1680/jgeen.16.00101>
- Sutton OF, Price JS (2020) Soil moisture dynamics modelling of a reclaimed upland in the early post-construction period. *Sci TOTAL ENVIRON* 718: 134628. <https://doi.org/10.1016/j.scitotenv.2019.134628>
- Taina IA, Heck RJ, Deen W, et al. (2013) Quantification of freeze-thaw related structure in cultivated topsoils using X-ray computer tomography. *Canadian Journal of Soil Science* 93(4SI): 533-553. <https://doi.org/10.4141/CJSS2012-044>
- Tang L, Cong S, Geng L, et al. (2018) The effect of freeze-thaw cycling on the mechanical properties of expansive soils. *Cold Regions Science and Technology* 145: 197-207. <https://doi.org/10.1016/j.coldregions.2017.10.004>
- Tang L, Cong S, Ling X, et al. (2018) A unified formulation of stress-strain relations considering micro-damage for expansive soils exposed to freeze-thaw cycles. *Cold Regions Science and Technology* 153: 164-171. <https://doi.org/10.1016/j.coldregions.2018.05.006>
- Tang L, Tian S, Ling X, et al. (2017) Effect of freeze-thaw cycles on the strength of base course materials used under China's high-speed railway line. *Cold Regions Science and Technology* 31(4): 06017003. [https://doi.org/10.1061/\(ASCE\)CR.1943-5495.0000125](https://doi.org/10.1061/(ASCE)CR.1943-5495.0000125)
- Tian L, Yu L, Liu S, et al. (2020) Deformation research of silty clay under freeze-thaw cycles. *KSCE Journal of Civil Engineering* 24(2): 435-442. <https://doi.org/10.1007/s12205-020-0987-0>
- Vahdani M, Ghazavi M, Roustaei M (2020) Measured and predicted durability and mechanical properties of frozen-thawed fine soils. *KSCE Journal of Civil Engineering* 24(3): 740-751. <https://doi.org/10.1007/s12205-020-2178-4>
- Wang D, Ma W, Chang X, et al. (2005) Physico-mechanical properties changes of Qinghai. *Chinese Journal of Rock Mechanics and Engineering* 24(23): 4313-4319 (in Chinese).
- Wang J, Jiang L, Cui H, et al. (2020) Evaluation and analysis of SMAP, AMSR2 and MEaSUREs freeze/thaw products in China. *Remote Sensing of Environment* 242: 111734. <https://doi.org/10.1016/j.rse.2020.111734>
- Wang J, Wang Q, Kong Y, et al. (2020) Analysis of the pore

- structure characteristics of freeze-thawed saline soil with different salinities based on mercury intrusion porosimetry. *Environmental Earth Sciences* 79(7): 161.
<https://doi.org/10.1007/s12665-020-08903-w>
- Wang L, Wang H, Tian Z, et al. (2020) Structural changes of compacted soil layers in northeast china due to freezing-thawing processes. *Sustainability* 12(4): 1587.
<https://doi.org/10.3390/su12041587>
- Wang M, Meng S, Sun Y, et al. (2018) Shear strength of frozen clay under freezing-thawing cycles using triaxial tests. *Earthq Eng Vib* 17(4): 761-769.
<https://doi.org/10.1007/s11803-018-0474-5>
- Wang R, Zhu D, Liu X, et al. (2015) Monitoring the freeze-thaw process of soil with different moisture contents using piezoceramic transducers. *Smart Mater Struct* 24(5): 057003.
<https://doi.org/10.1088/0964-1726/24/5/057003>
- Wang S, Wang Q, Xu J, et al. (2020) Effect of freeze-thaw on freezing point and thermal conductivity of loess. *Arab J Geosci* 13(5): 206.
<https://doi.org/10.1007/s12517-020-5186-2>
- Wang S, Yang P, Dai D, et al. (2020) A study on micro-pore characteristics of clay due to freeze-thaw and compression by mercury intrusion porosimetry. *Front Earth Sci* 7: 344.
<https://doi.org/10.3389/feart.2019.00344>
- Wang T, Li P, Li Z, et al. (2019) The effects of freeze-thaw process on soil water migration in dam and slope farmland on the Loess Plateau, China. *Science of the Total Environment* 666: 721-730.
<https://doi.org/10.1016/j.scitotenv.2019.02.284>
- Wei C, Apel DB, Zhang Y (2019) Shear behavior of ultrafine magnetite tailings subjected to freeze-thaw cycles. *Int J Ming Sci Technol* 29(4SI): 609-616.
<https://doi.org/10.1016/j.ijmst.2019.06.007>
- Wu X, Wang F, Li T, et al. (2020) Nitrogen additions increase N₂O emissions but reduce soil respiration and CH₄ uptake during freeze-thaw cycles in an alpine meadow. *Geoderma* 363: 114157. <https://doi.org/10.1016/j.geoderma.2019.114157>
- Xian S, Lu Z, Yao H, et al. (2019) Comparative study on mechanical properties of compacted clay under freeze-thaw cycles with closed and open systems. *Adv Mater Sci Eng* 2019: 9206372. <https://doi.org/10.1155/2019/9206372>
- Xie S, Qu J, Lai Y, et al. (2015) Effects of freeze-thaw cycles on soil mechanical and physical properties in the Qinghai-Tibet Plateau. *J Mt Sci* 12(4): 999-1009.
<https://doi.org/10.1007/s11629-014-3384-7>
- Xu J, Li Y, Lan W, et al. (2019) Shear strength and damage mechanism of saline intact loess after freeze-thaw cycling. *Cold Reg Sci Technol* 164: UNSP 102779.
<https://doi.org/10.1016/j.coldregions.2019.05.005>
- Xu J, Wang Z, Ren J, et al. (2018) Mechanism of slope failure in loess terrains during spring thawing. *J Mt Sci* 15(4): 845-858.
<https://doi.org/10.1007/s11629-017-4584-8>
- Yang C, Wu T, Yao J, et al. (2020) An assessment of using remote sensing-based models to estimate ground surface soil heat flux on the tibetan plateau during the freeze-thaw process. *Remote Sens* 12(3): 501.
<https://doi.org/10.3390/rs12030501>
- Yang Z, Li X, Li D, et al. (2020) Effects of long-term repeated freeze-thaw cycles on the engineering properties of compound solidified/stabilized pb-contaminated soil: deterioration characteristics and mechanisms. *Int J Env Res Pub Health* 17(5): 1798. <https://doi.org/10.3390/ijerph17051798>
- Yang Z, Wang Y, Li D, et al. (2020) Influence of freeze-thaw cycles and binder dosage on the engineering properties of compound solidified/stabilized lead-contaminated soils. *Int J Env Res Pub Health* 17(3): 1077.
<https://doi.org/10.3390/ijerph17031077>
- Yao X, Fang L, Qi J, et al. (2017) Study on mechanism of freeze-thaw cycles induced changes in soil strength using electrical resistivity and x-ray computed tomography. *J Offshore Mech Arct Eng Trans ASME* 139(2): 021501.
<https://doi.org/10.1115/1.4035244>
- Ye WJ, Wei We, Zheng C, et al. (2019) Effect of initial moisture content on mechanical properties of expansive paleosol. *J Civ Eng Manag* 36(4): 28-32 (in Chinese).
<https://doi.org/10.13579/j.cnki.2095-0985.2019.04.005>
- Yuan L, Zhao L, Li R, et al. (2020) Spatiotemporal characteristics of hydrothermal processes of the active layer on the central and northern Qinghai-Tibet plateau. *Sci Total Environ* 712: 136392.
<https://doi.org/10.1016/j.scitotenv.2019.136392>
- Zhang M, Zhang X, Lai Y, et al. (2020) Variations of the temperatures and volumetric unfrozen water contents of fine-grained soils during a freezing-thawing process. *Acta Geotech* 15(3): 595-601.
<https://doi.org/10.1007/s11440-018-0720-z>
- Zhang S, Liu H, Chen W, et al. (2020) Strength deterioration model of remolded loess contaminated with acid and alkali solution under freeze-thaw cycles. *Bull Eng Geol Environ*.
<https://doi.org/10.1007/s10064-019-01721-w>
- Zhang S, Qu F, Wang X, et al. (2020) Freeze-thaw cycles changes soil nitrogen in a Mollisol sloping field in Northeast China. *Nutr Cycl Agroecosyst* 116(3): 345-364.
<https://doi.org/10.1007/s10705-020-10048-y>
- Zhang S, Wang X, Xiao Z, et al. (2020) Quantitative studies of gully slope erosion and soil physiochemical properties during freeze-thaw cycling in a Mollisol region. *Sci Total Environ* 707(136191).
<https://doi.org/10.1016/j.scitotenv.2019.136191>
- Zhang W, Guo A, Lin C (2019) Effects of cyclic freeze and thaw on engineering properties of compacted loess and lime-stabilized loess. *J Mater Civil Eng* 31: 040192059.
<https://doi.org/10.1016/j.scitotenv.2019.136191>
- Zhang W, Ma J, Tang L (2019) Experimental study on shear strength characteristics of sulfate saline soil in Ningxia region under long-term freeze-thaw cycles. *Cold Reg Sci Technol* 160: 48-57.
<https://doi.org/10.1016/j.coldregions.2019.01.008>
- Zhang Y, Daniels JL, Cetin B, et al. (2020) Effect of temperature on pH, conductivity, and strength of lime-stabilized soil. *J Mater Civil Eng* 32(3): 04019380.
[https://doi.org/10.1061/\(ASCE\)MT.1943-5533.0003062](https://doi.org/10.1061/(ASCE)MT.1943-5533.0003062)
- Zhang Z, Cui Z (2017) Analysis of microscopic pore structures of the silty clay before and after freezing-thawing under the subway vibration loading. *Environ Earth Sci* 76(15): 528.
<https://doi.org/10.1007/s12665-017-6879-z>
- Zhang Z, Cui Z (2018) Effects of freezing-thawing and cyclic loading on pore size distribution of silty clay by mercury intrusion porosimetry. *Cold Reg Sci Technol* 145: 185-196.
<https://doi.org/10.1016/j.coldregions.2017.11.002>
- Zhao L, Sun M, Sun H, et al. (2018) Discharge simulation and sensitivity to climate change of the Kuytun River Basin on the north slope of Tianshan Mountains, China. *Mt Res Dev* 36(5): 722-730. (in Chinese)
<https://doi.org/10.16089/j.cnki.1008-2786.000368>
- Zhen Z, Ma G, Zhang H, et al. (2019) Thermal conductivities of remolded and undisturbed loess. *J Mater Civil Eng* 31(2): 04018379.
[https://doi.org/10.1061/\(ASCE\)MT.1943-5533.0002595](https://doi.org/10.1061/(ASCE)MT.1943-5533.0002595)
- Zhou Z, Liu Z, Yang H, et al. (2020) Freeze-thaw damage mechanism of elastic modulus of soil-rock mixtures at different confining pressures. *J Cent South Univ* 27(2): 554-565.
<https://doi.org/10.1007/s11771-020-4316-z>
- Zhou Z, Ma W, Zhang S, et al. (2020) Experimental investigation of the path-dependent strength and deformation behaviours of frozen loess. *Eng Geol* 265: 105449.
<https://doi.org/10.1016/j.enggeo.2019.105449>
- Zhou Z, Xing K, Yang H, et al. (2019) Damage mechanism of soil-rock mixture after freeze-thaw cycles. *J Cent South Univ* 26(1): 13-24.
<https://doi.org/10.1007/s11771-019-3979-9>